Electronic Supplementary Information

Impact of charge transport layers on photochemical stability of $MAPbI_3$ in thin films and perovskite solar cells

A. G. Boldyreva*[a], A. F. Akbulatov[b], M. Elnaggar[a, c], S. Yu. Luchkin[a], A. V. Danilov[d], I. S. Zhidkov[e], O. R. Yamilova[a,b], Yu. S. Fedotov[d], S. I. Bredikhin[d], E. Z. Kurmaev[e,f], K. J. Stevenson[a], and P. A. Troshin[a,b]

[a] *Skolkovo Institute of Science and Technology, Nobel street 3, Moscow, 143026, Russia.*
[b] *Institute for Problems of Chemical Physics of the Russian Academy of Sciences (ICP RAS), Semenov prospect 1, Chernogolovka, 142432, Moscow region, Russia*
[c] *Moscow Institute of Physics and Technology, Dolgoprudny, 141700, Moscow region, Russia*
[d] *Institute of Solid State Physics of Russian Academy of Science (ISSP RAS), Chernogolovka, 142432 Moscow region, Russia*
[e] *Institute of Physics and Technology, Ural Federal University, Mira 9 str., 620002, Yekaterinburg, Russia*
[f] *M.N.Mikheev Institute of Metal Physics of Ural Branch of Russian Academy of Sciences, S. Kovalevskoi 18 str., 620108 Yekaterinburg, Russia*
**Corresponding author: aleksandra.boldyreva@skolkovotech.ru*

Contents

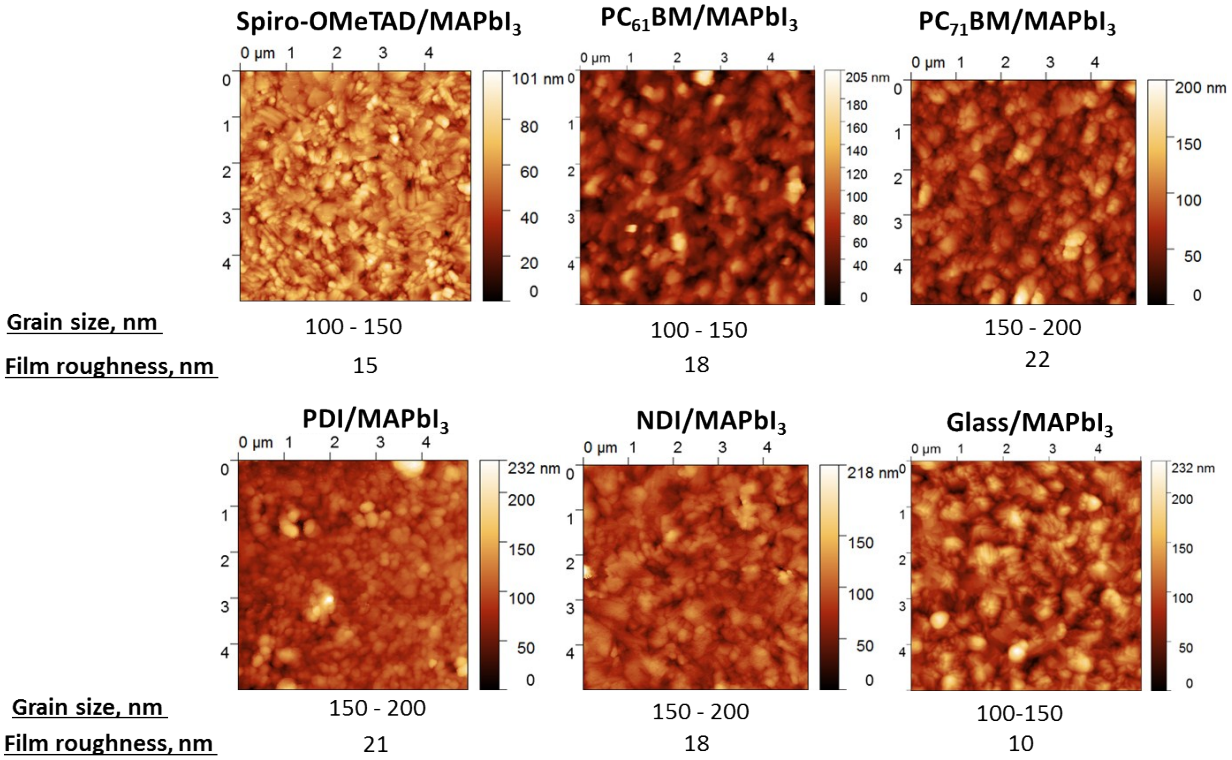

Figure S1. AFM surface topography of CTL/$MAPbI_3$ films before light soaking

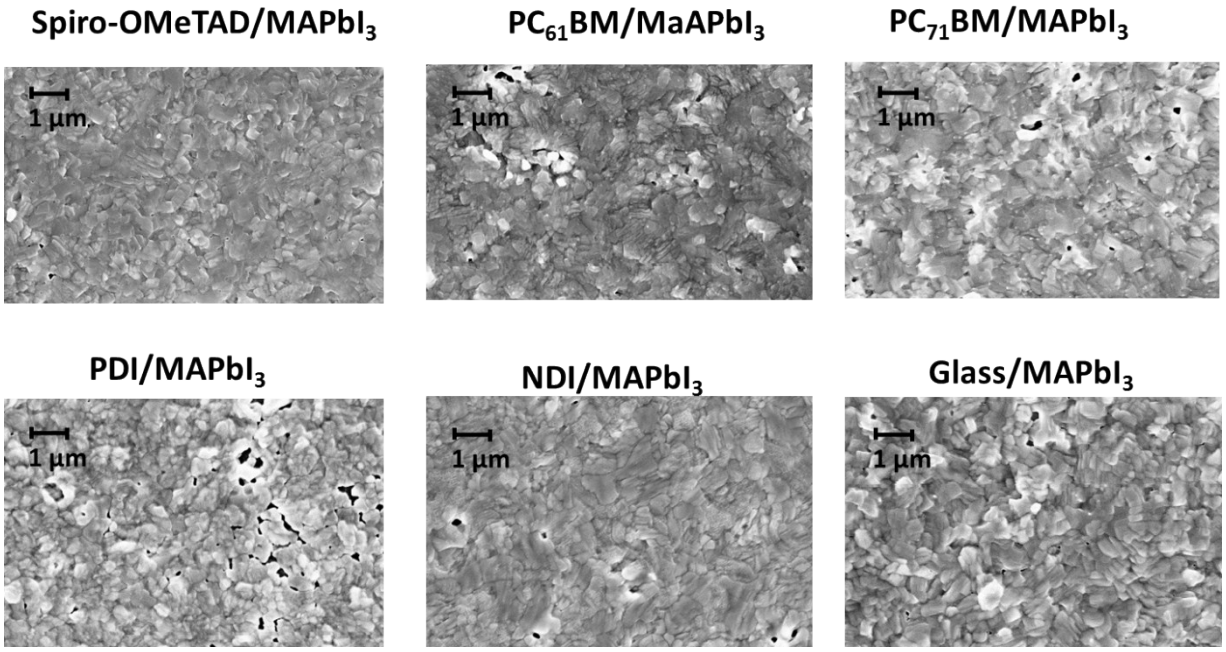

Figure S2. SEM images of CTL/$MAPbI_3$ films before light soaking

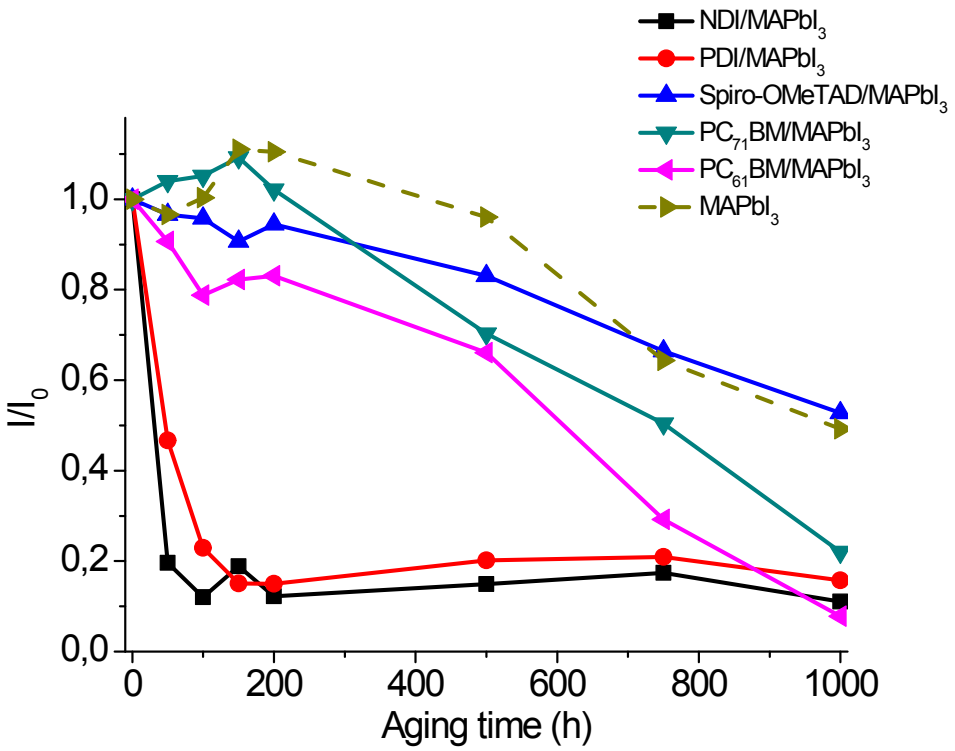

Figure S3. Evolution of the optical density of glass/CTL/$MAPbI_3$ stacks at 700 nm (I_0 stands for initial optical density at this wavelength).

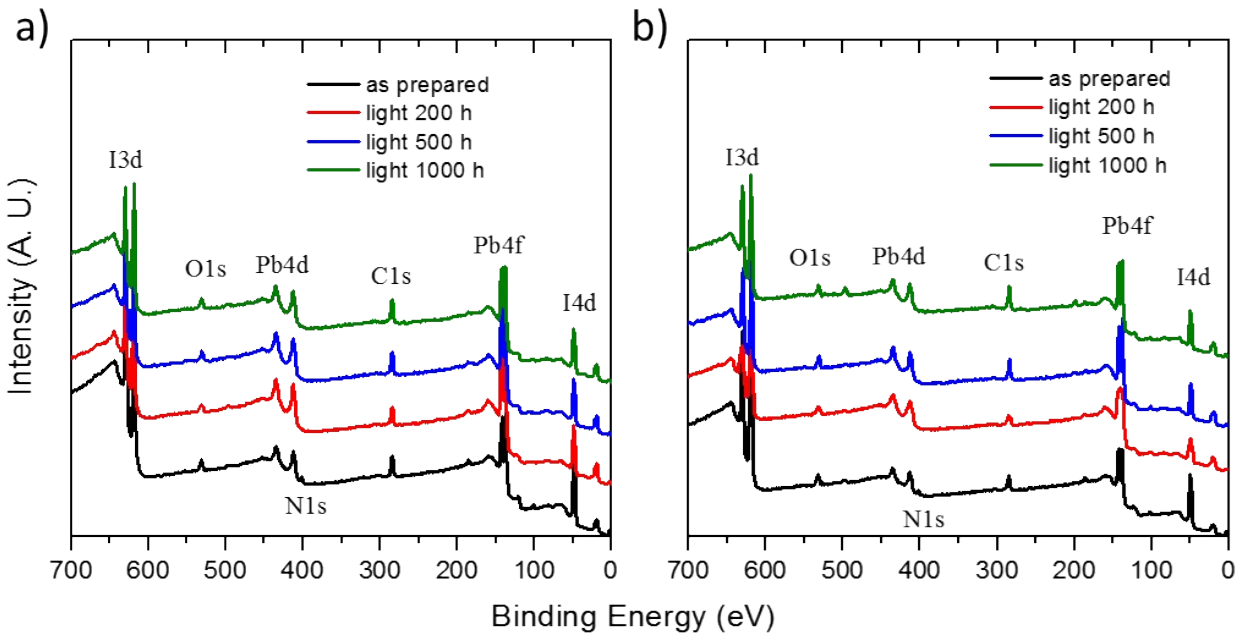

Figure S4. Evolution of the XPS survey spectra of glass/NDI/$MAPbI_3$ (a) and glass/PDI/$MAPbI_3$ (b) stacks under light soaking conditions.

Table S1. Surface composition (in at.%) of glass/NDI/$MAPbI_3$ and glass/PDI/$MAPbI_3$ samples estimated from XPS spectra.

Configuration	Aging time (h)	Surface composition (at. %)			Element ratio	
		N	Pb	I	I:Pb	N:Pb
NDI/$MAPbI_3$	0	6.1	9.7	23.8	2.45	0.62
	500	1.7	7.4	16.3	2.20	0.22
	1000	0.9	11.1	14.4	1.29	0.08
PDI/$MAPbI_3$	0	7.5	8.6	21.7	2.52	0.87
	500	0	10.3	13.1	1.27	0
	1000	0	8.6	12.5	1.45	0

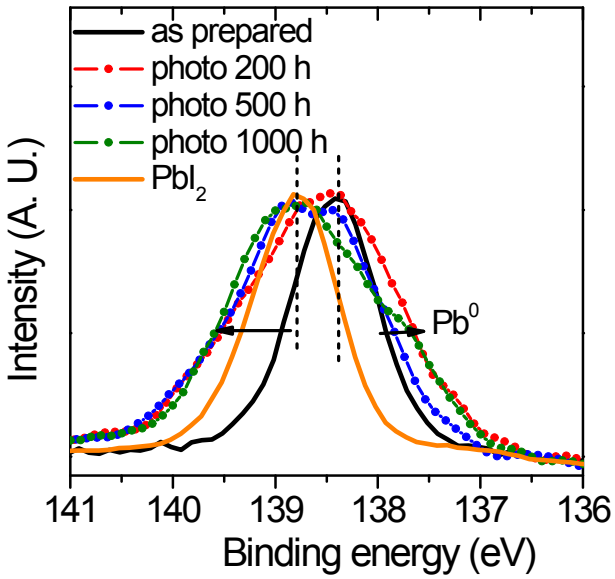

Figure S5. Evolution of the XPS Pb $4f_{7/2}$ band for glass/PDI/$MAPbI_3$ stacks under light soaking conditions.

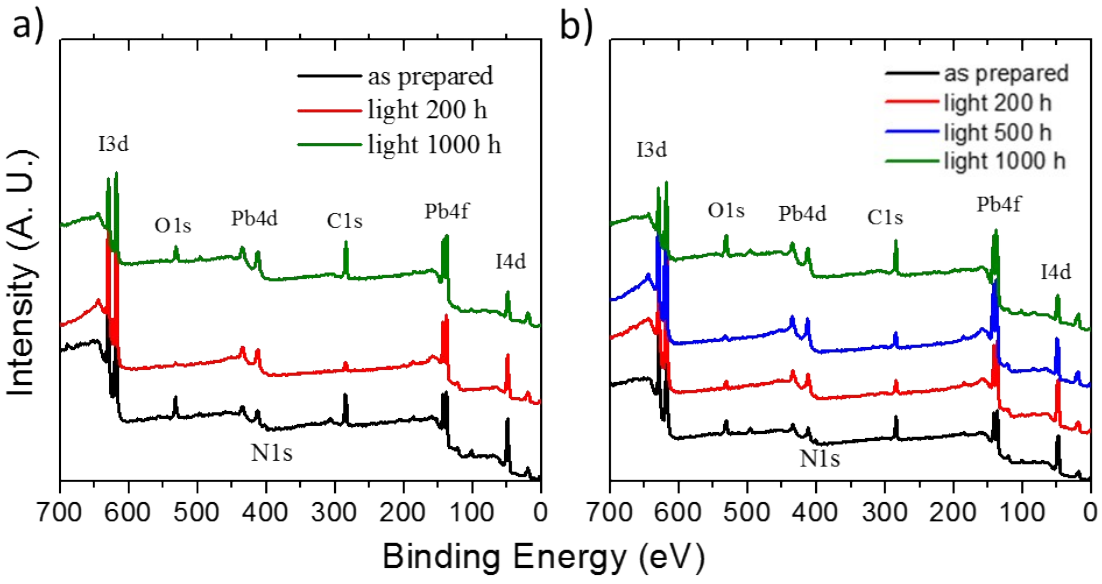

Figure S6. Evolution of the XPS survey spectra of glass/$PC_{61}BM$/$MAPbI_3$ (a) and glass/$PC_{71}BM$/$MAPbI_3$ (b) samples under light soaking conditions.

Table S2. Surface composition (in at.%) of $PC_{61}BM/MAPbI_3$ and $PC_{71}BM/MAPbI_3$ samples estimated from XPS spectra

Configuration	Aging time (h)	Surface composition (at. %)			Element Ratio	
		N	Pb	I	I:Pb	N:Pb
$PC_{61}BM/MAPbI_3$	0	4.1	4.3	11.9	2.76	0.95
	200	3.8	15.6	32.2	2.06	0.24
	500	0	0.1	0.2	1.0	0
	1000	0	6.8	6.7	0.98	0
$PC_{71}BM/MAPbI_3$	0	3.8	5.7	12.7	2.22	0.66
	200	5.7	11.8	24	2.03	0.48
	500	0	13.5	19.1	1.41	0
	1000	0	7.3	6.4	0.87	0

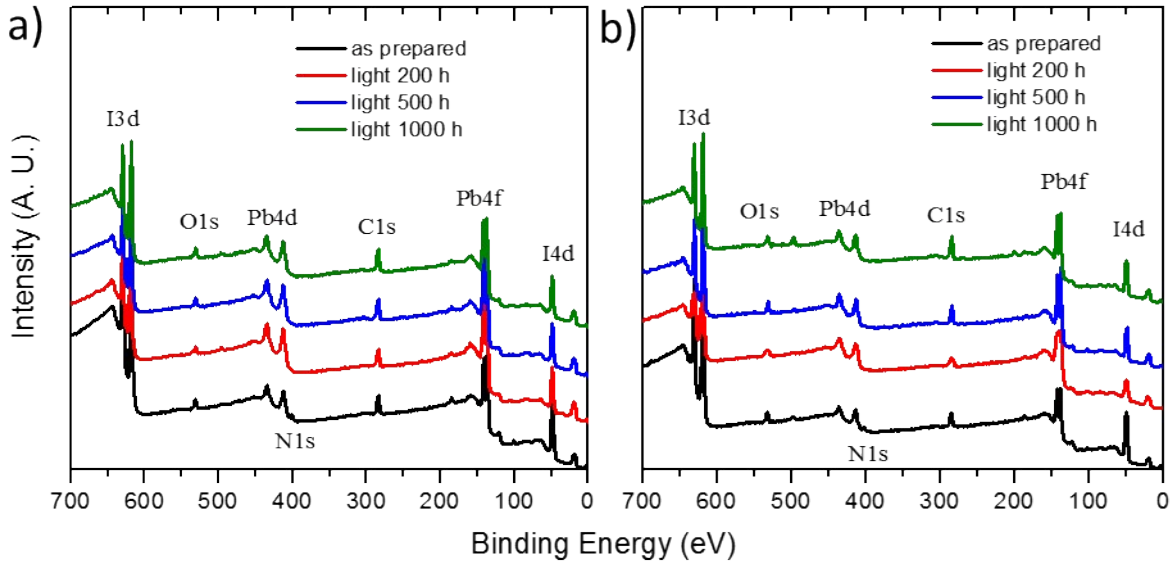

Figure S7. XPS survey spectra of spiro-OMeTAD/$MAPbI_3$ (a) and pristine $MAPbI_3$ (b) samples before and after light illumination.

Table S3. Surface composition (in at.%) of spiro-OMeTAD/$MAPbI_3$ (a) and pristine $MAPbI_3$ (b) samples estimated from XPS spectra.

Configuration	Aging time (h)	Surface composition (at. %)			Element ratio	
		N	Pb	I	I:Pb	N:Pb
Spiro-OMeTAD/$MAPbI_3$	0	7.7	9.6	25.1	2.61	0.80
	200	7.8	10.8	24.4	2.25	0.72
	500	0	15.2	24.7	1.62	0
	1000	0	13.2	19.1	1.44	0
$MAPbI_3$	0	6.8	9.5	25.3	2.66	0.71
	200	6.2	11	26.5	2.40	0.56
	500	0	14.8	21.1	1.42	0
	1000	0	15.5	19.9	1.28	0

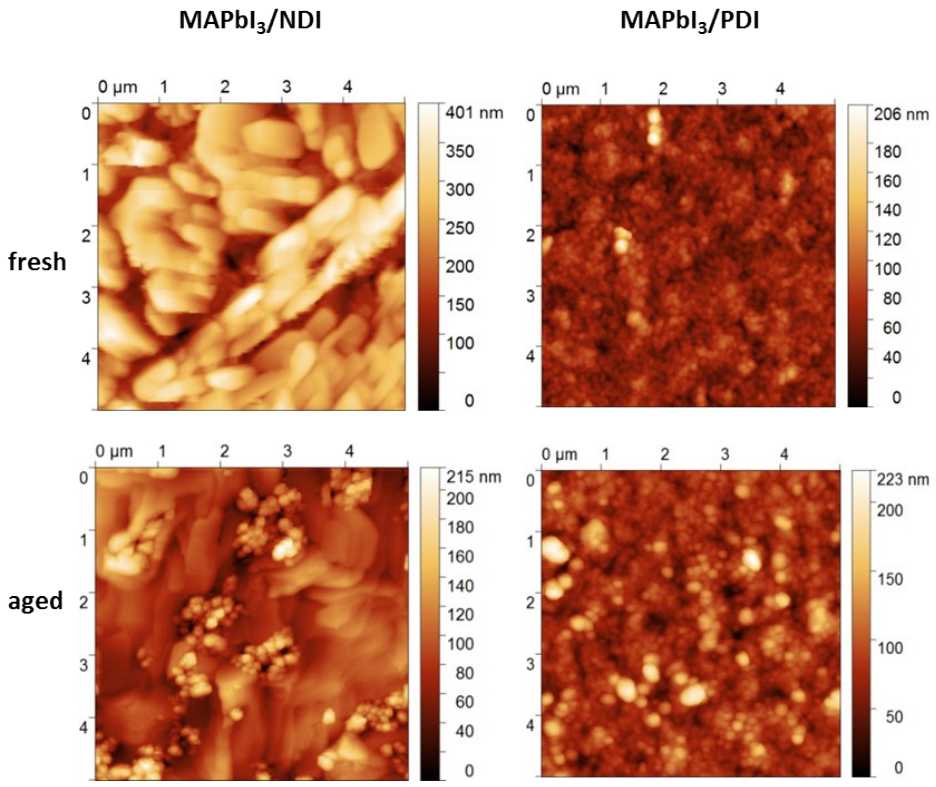

Figure S8. Surface topography of glass/$MAPbI_3$/NDI and glass/$MAPbI_3$/PDI films before and after 1000 h exposure to the light soaking.

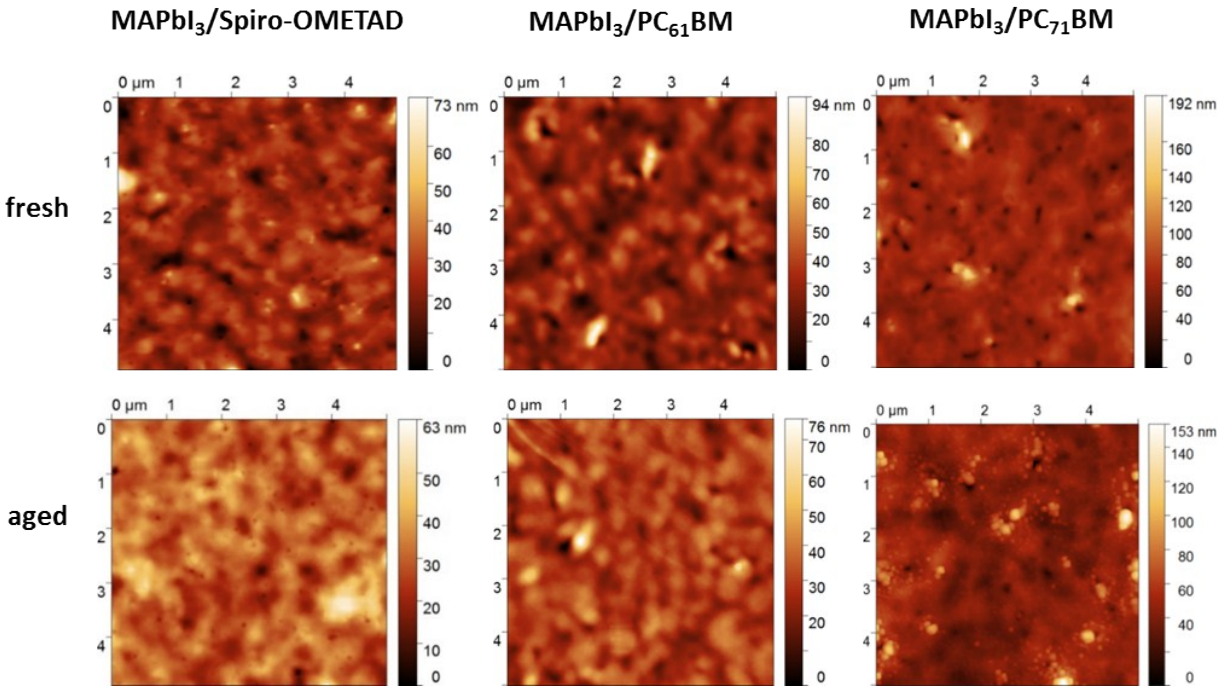

Figure S9. Surface topography of glass/$MAPbI_3$/Spiro-OMeTAD, glass/$MAPbI_3$/$PC_{61}BM$ and glass/$MAPbI_3$/$PC_{71}BM$ films before and after 1000 h exposure to the light soaking.

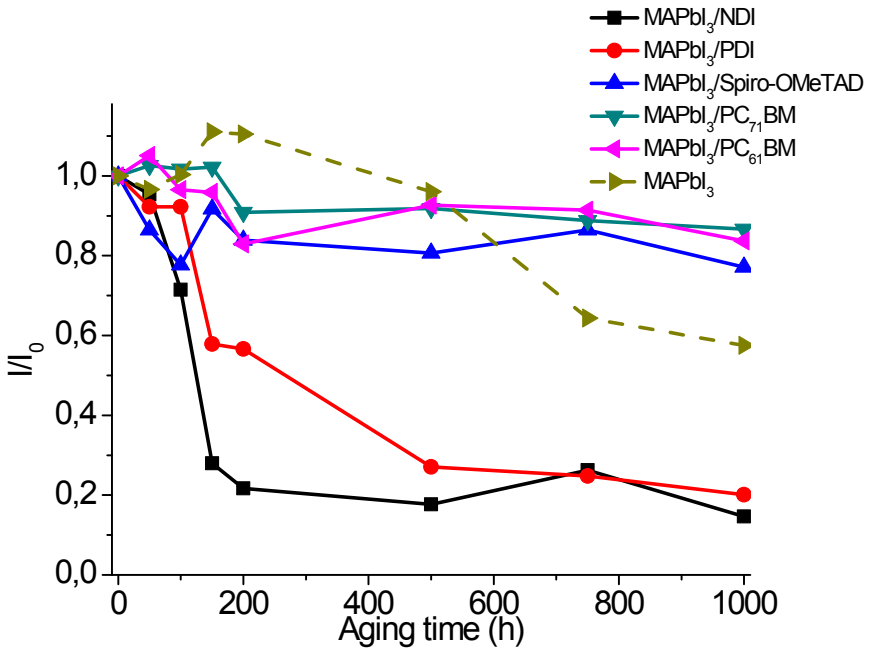

Figure S10. Evolution of the optical density of glass/$MAPbI_3$/CTL stacks at 700 nm (I_0 stands for initial optical density at this wavelength).

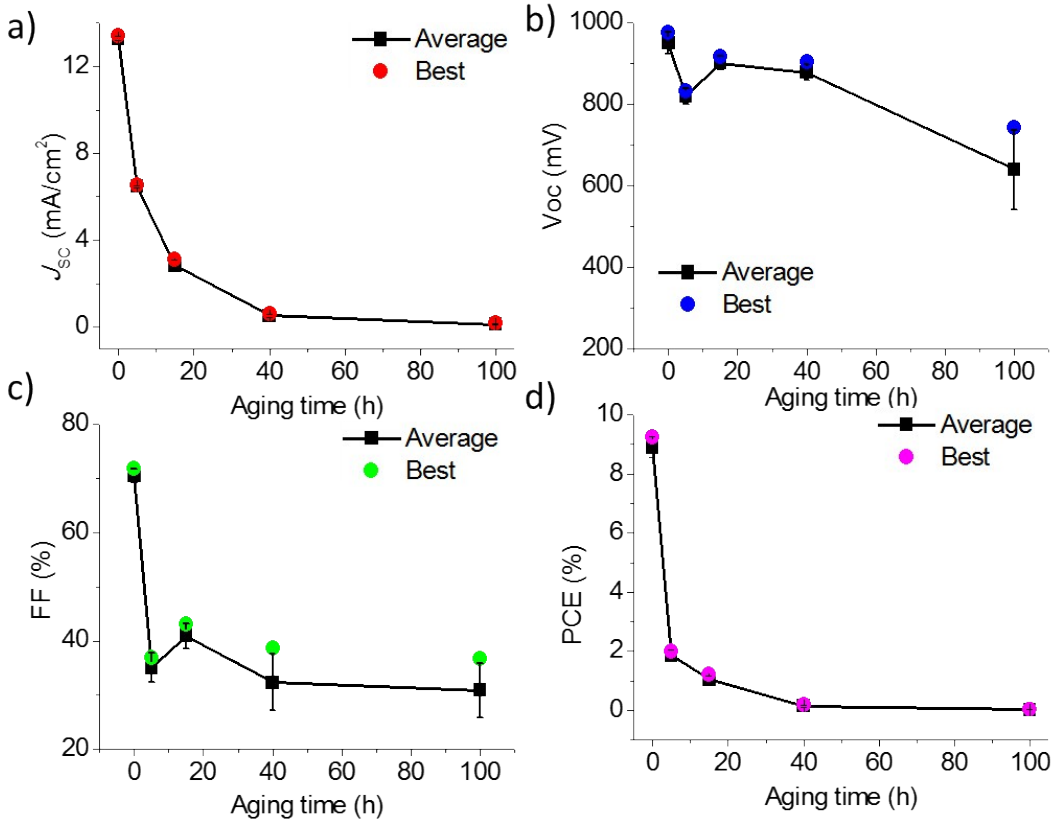

Figure S11. Evolution of the characteristics of ITO/PEDOT:PSS/$MAPbI_3$/$PC_{61}BM$/Mg/Ag solar cells under light soaking conditions applied to ITO/PEDOT:PSS/$MAPbI_3$/$PC_{61}BM$ stacks: short circuit current density J_{SC} (a), open circuit voltage V_{OC} (b), fill factor FF (c) and power conversion efficiency PCE (d).

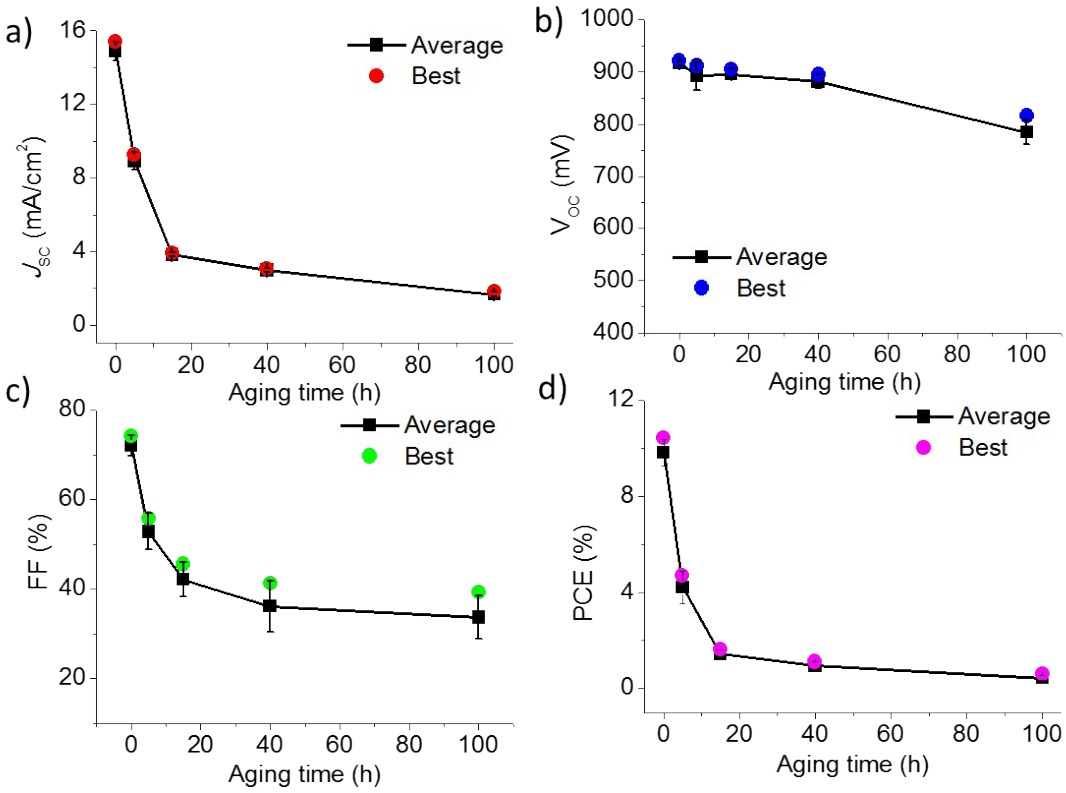

Figure S12. Evolution of the characteristics of ITO/PEDOT:PSS/$MAPbI_3$/$PC_{71}BM$/Mg/Ag solar cells under light soaking conditions applied to ITO/PEDOT:PSS/$MAPbI_3$/$PC_{71}BM$ stacks: short circuit current density J_{SC} (a), open circuit voltage V_{OC} (b), fill factor FF (c) and power conversion efficiency PCE (d).

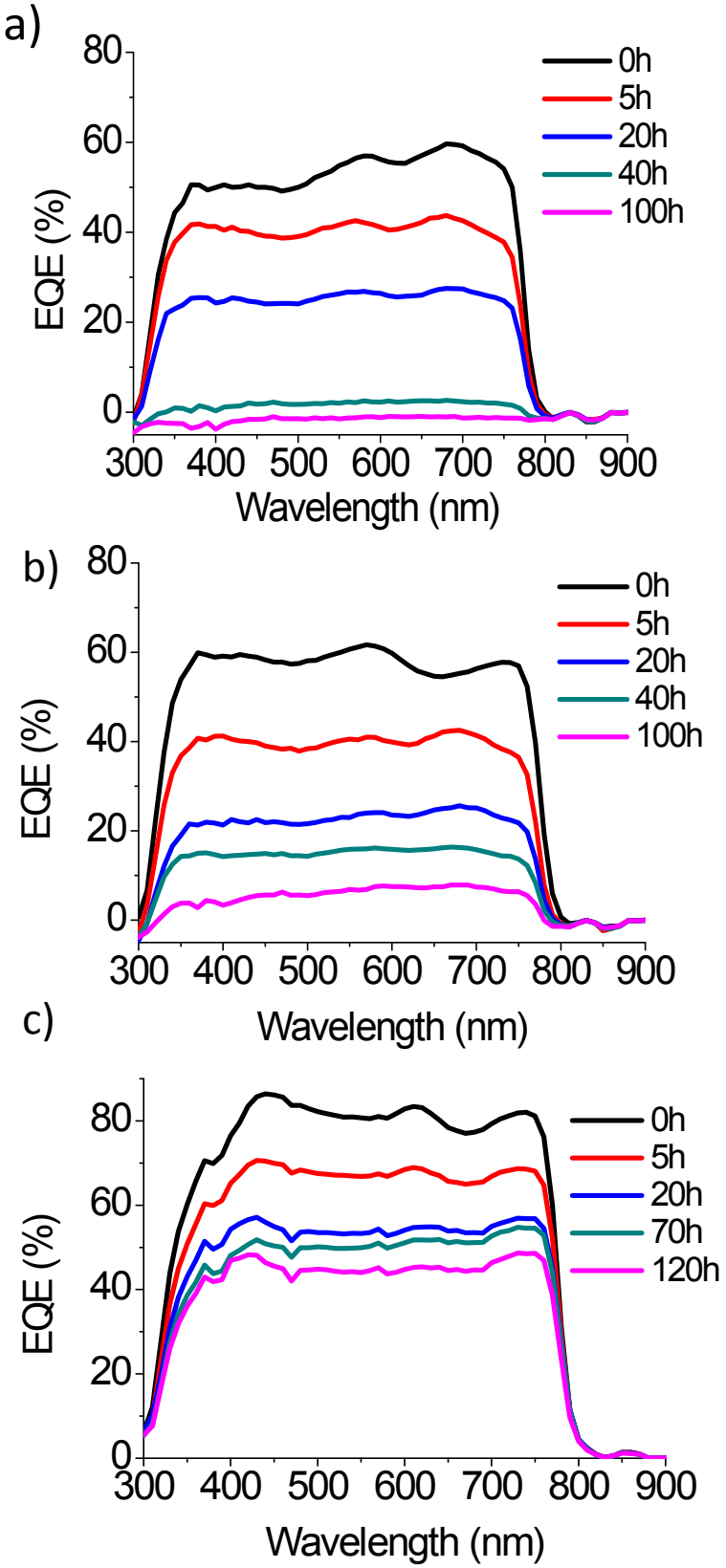

Figure S13. Evolution of EQE spectra of ITO/PEDOT:PSS/$MAPbI_3$/$PC_{61}BM$/Mg/Ag (a), ITO/PEDOT:PSS/$MAPbI_3$/$PC_{71}BM$/Mg/Ag (b) and ITO/SnO_2/$MAPbI_3$/spiro-OMeTAD/Ag/Au (c) solar cells fabricated using fresh and exposed to light soaking top electrode free stacks

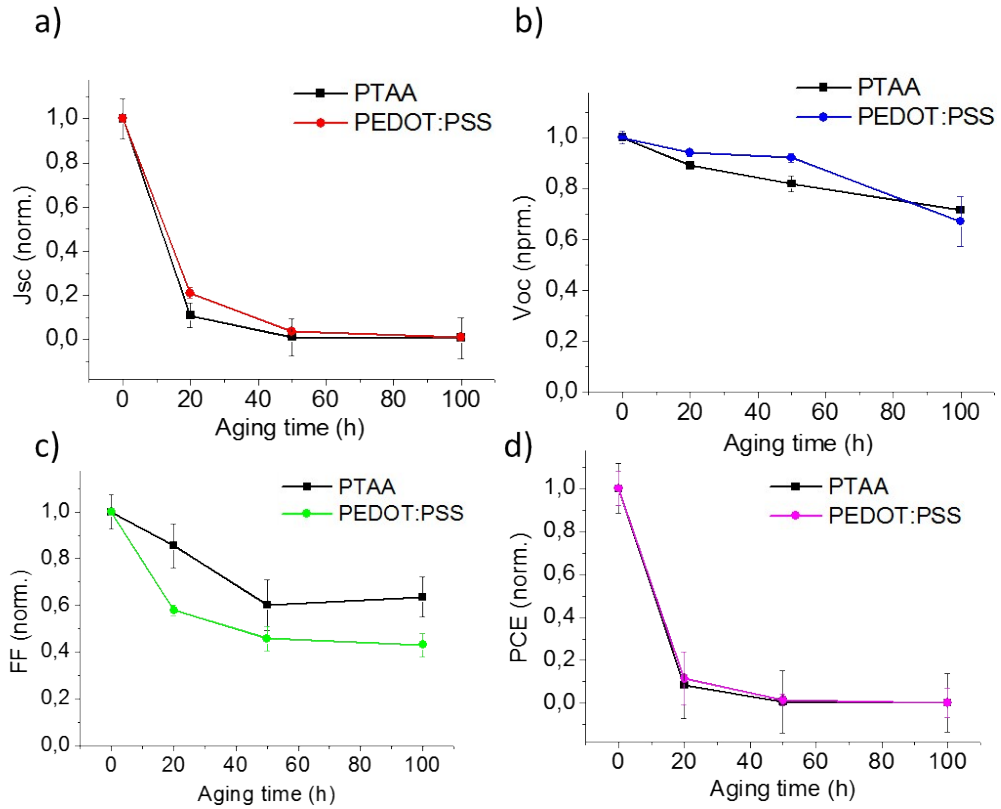

Figure S14. Comparison of the degradation behavior of ITO/PEDOT:PSS/$MAPbI_3$/$PC_{61}BM$/Mg/Ag and ITO/PTAA/$MAPbI_3$/$PC_{61}BM$/Mg/Ag solar cells under light soaking conditions applied to the electrode-free stacks: short circuit current density J_{SC} (a), open circuit voltage V_{OC} (b), fill factor FF (c) and power conversion efficiency PCE (d).

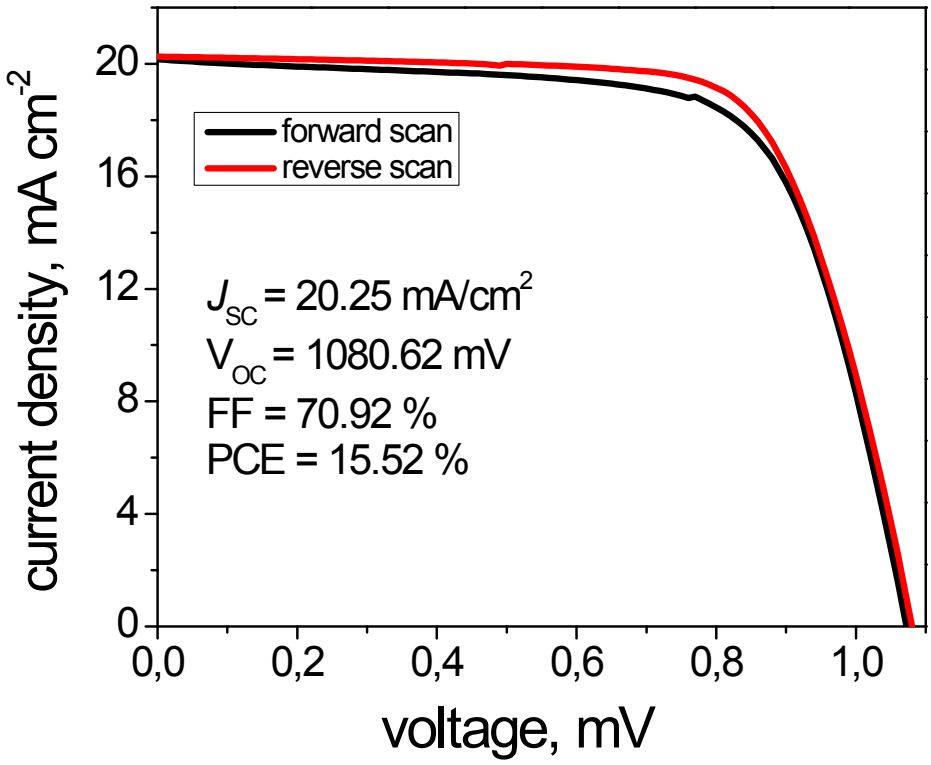

Figure S15. IV characteristics of ITO/PTAA/$MAPbI_3$/$PC_{61}BM$/Mg/Ag solar cell

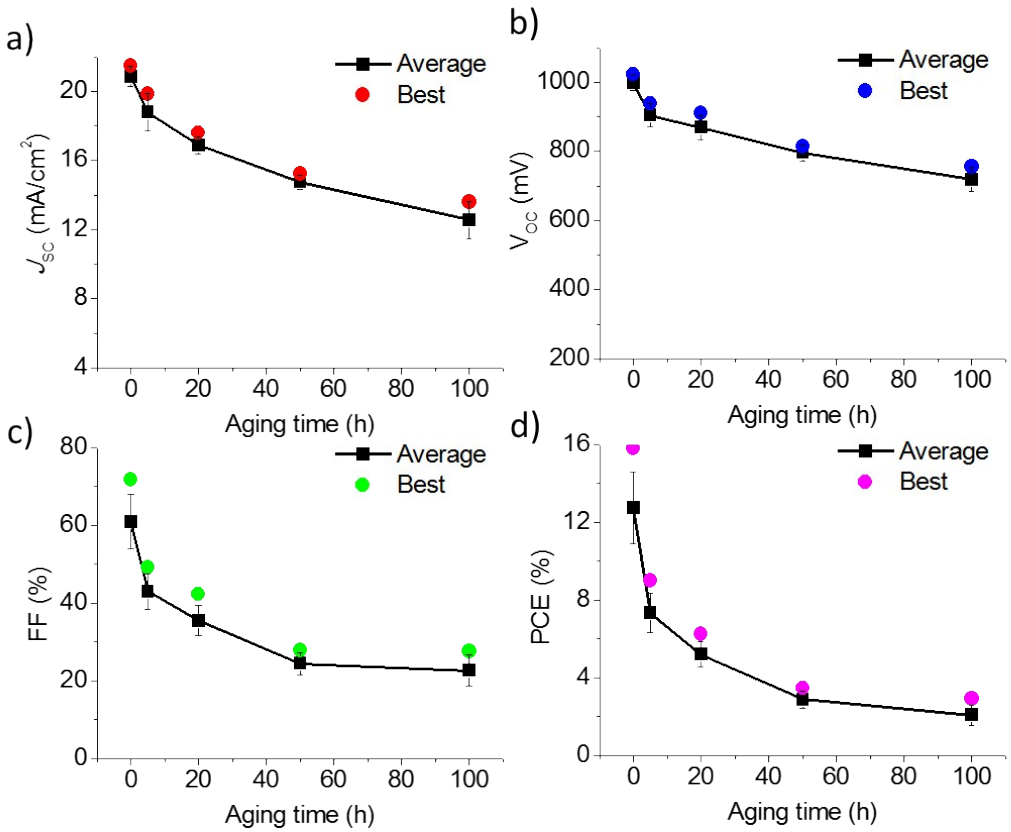

Figure S16. Evolution of the characteristics of ITO/SnO_2/$MAPbI_3$/Spiro-OMeTAD/Ag/Au solar cells under light soaking conditions applied to ITO/SnO_2/$MAPbI_3$/Spiro-OMeTAD stacks: short circuit current density J_{SC} (a), open circuit voltage V_{OC} (b), fill factor FF (c) and power conversion efficiency PCE (d).